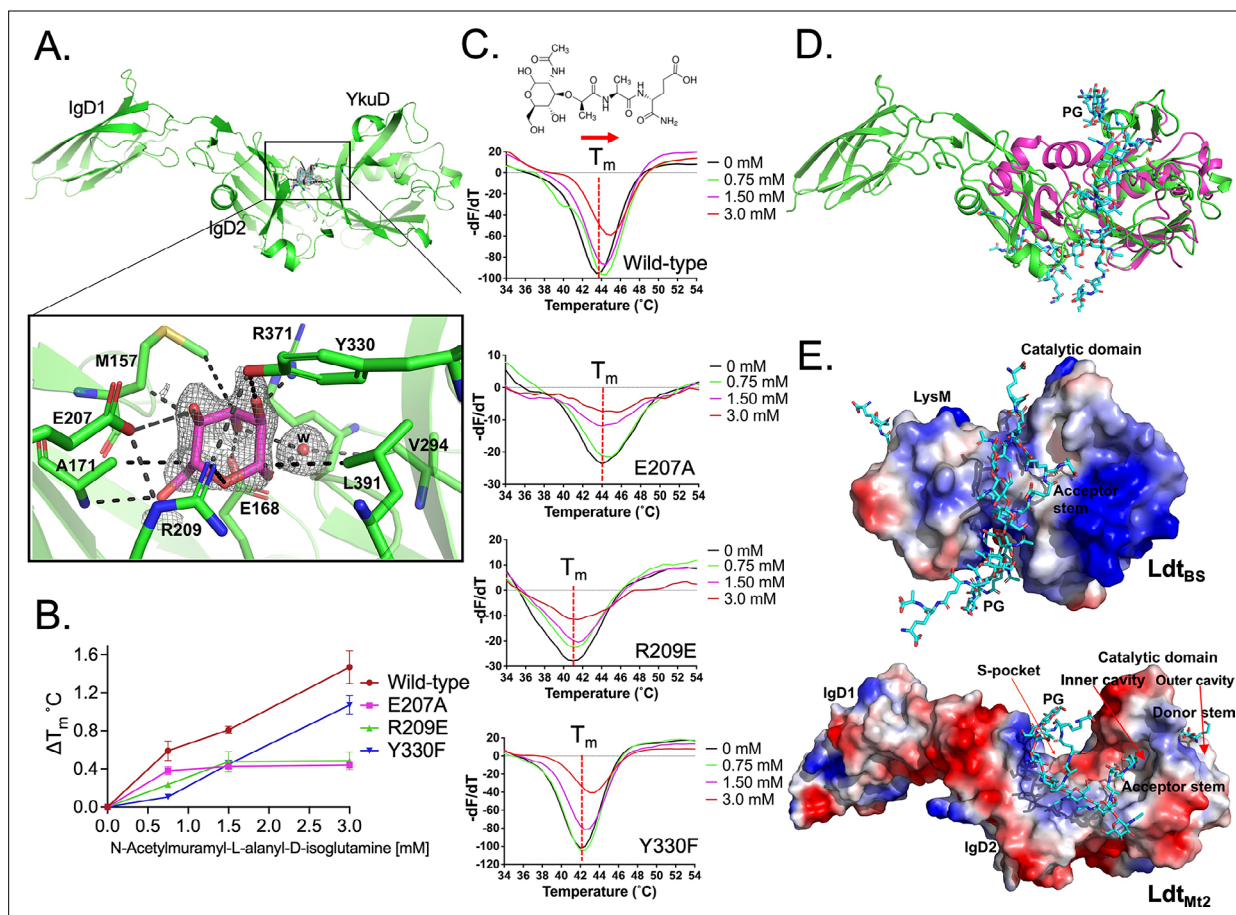


---

## Figures and figure supplements

Allosteric cooperation in  $\beta$ -lactam binding to a non-classical transpeptidase

**Nazia Ahmad et al**



**Figure 1.** Binding studies of peptidoglycan (PG) with  $Ldt_{M12}$ . **(A)** Crystal structure of  $Ldt_{M12}$  in complex with one glucose molecule. The inset shows the  $2F_o - F_c$  omit map (contoured at  $1.0\sigma$ ) of glucose (cyan colour) modelled into the S-pocket of  $Ldt_{M12}$  in the crystal structure. **(B)** ThermoFluor assay for binding studies with the PG-precursor *N*-acetylmuramyl-L-alanyl-D-isoglutamine hydrate with wild-type  $Ldt_{M12}$ , R209E, E207A, and Y330F mutants. A change in melting temperature ( $\Delta T_m$ ) at y-axis was plotted against the ligand concentrations at x-axis in GraphPad Prism software. **(C)** Differential fluorescence ( $-dF/dT$ ) graphs of ThermoFluor assay for  $Ldt_{M12}$  and mutants. The dotted line indicates the  $T_m$ , and a red arrow indicates the direction of thermal shift. A chemical structure above the ThermoFluor assay graph is *N*-acetylmuramyl-L-alanyl-D-isoglutamine hydrate. **(D)** Superposition of  $Ldt_{M12}$  (green) with PG-bound  $Ldt_{B5}$ , the *Bacillus subtilis* L,D-transpeptidase (PDB ID: 2MTZ) (pink). YkuD domain of  $Ldt_{M12}$  was superposed with catalytic domain of  $Ldt_{B5}$  with an RMSD of 1.46 Å. PG chain is shown in cyan colour. **(E)** Modelling of PG (cyan colour) into the  $Ldt_{M12}$  (green). Electrostatic potential (negative in red, positive in blue) highlights the acidic and positively charge surface and binding of PG chain in L,D-transpeptidases  $Ldt_{B5}$  and  $Ldt_{M12}$ .

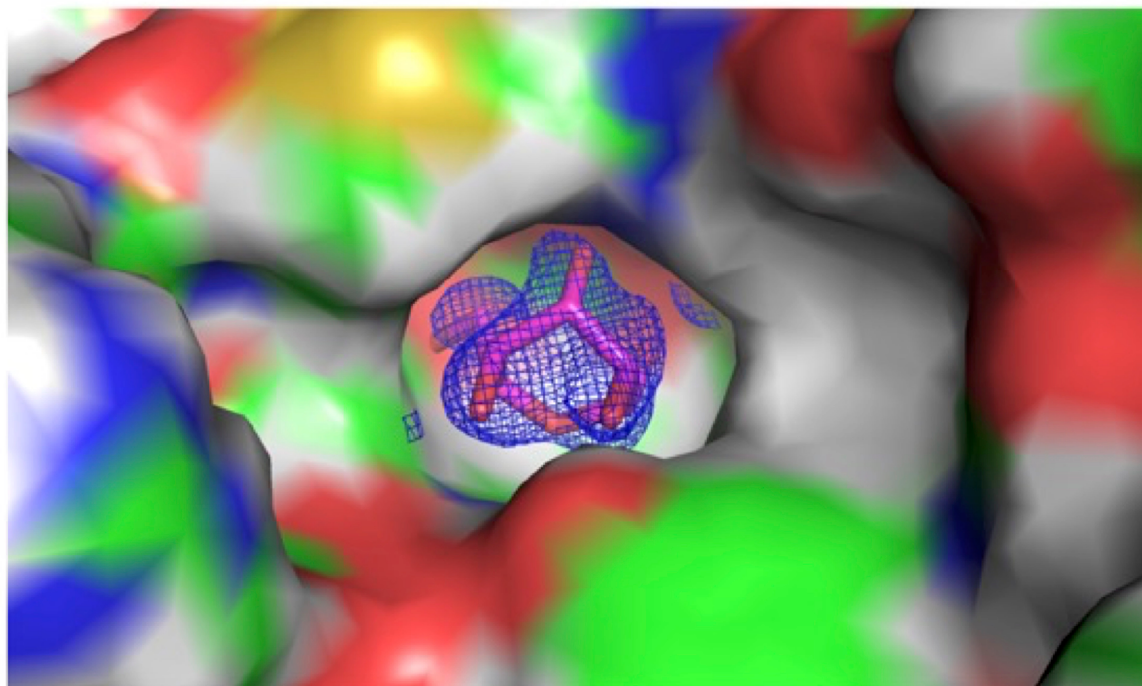


**Figure 1—figure supplement 1.** 2Fo-Fc map of sugar bound into the S-pocket of Ldt<sub>M12</sub> in the crystal structure. S-pocket is represented in surface. Sugar is shown in stick model in pink colour. 2Fo-Fc map is shown in blue colour and contoured at 1.0σ.

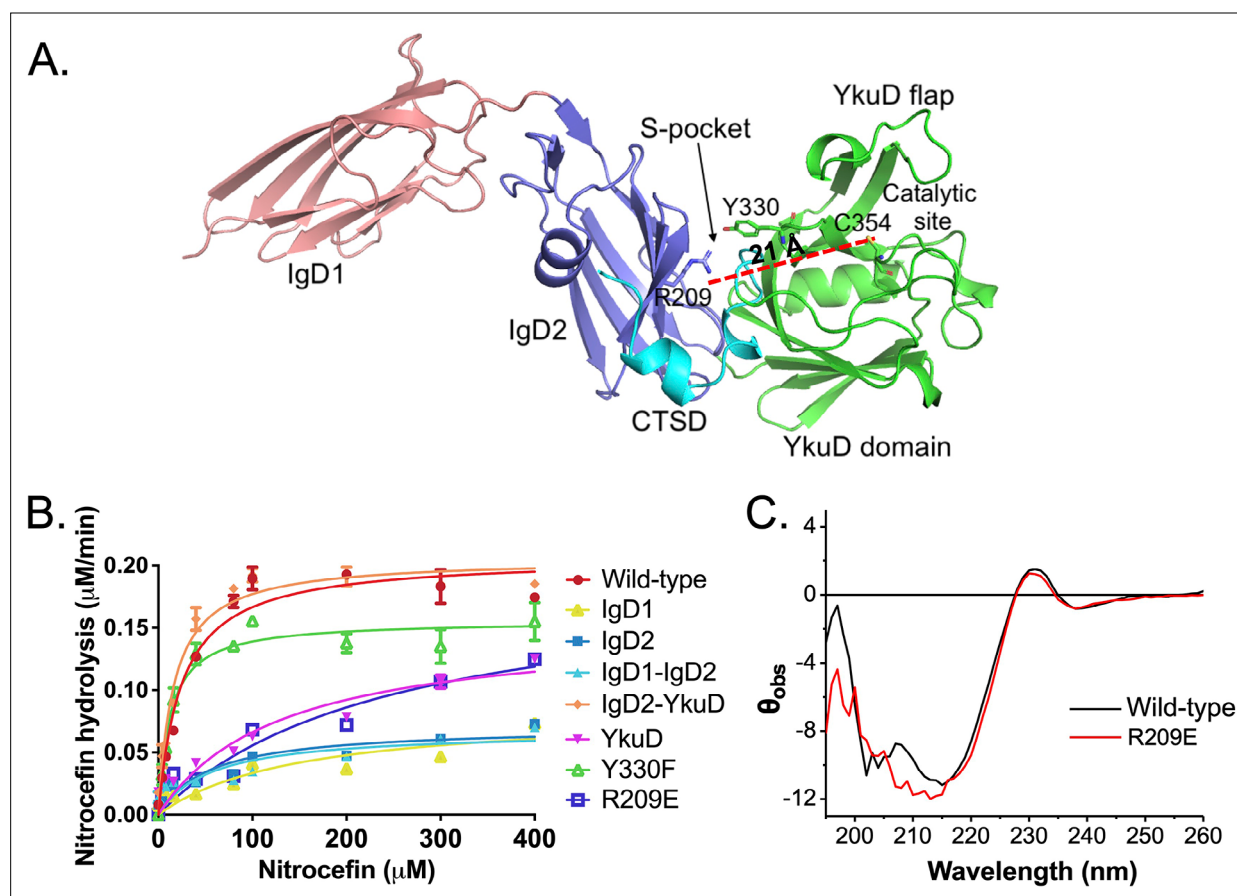


**Figure 2.** Role of the S-pocket in  $\beta$ -lactam hydrolysis. **(A)** The structure of Ldt<sub>M12</sub> with each domain highlighted: IgD1 (orange), IgD2 (blue), YkuD domain (green), and C-terminal subdomain (CTSD) (cyan). A red dotted line demarcates the 21 Å distance between the S-pocket and the catalytic site. **(B)** Chromogenic nitrocefin hydrolysis activity of truncated Ldt<sub>M12</sub> fragments corresponding to the IgD1, IgD2, IgD1-IgD2, YkuD, IgD2-YkuD domains, R209E, and Y330F mutants. **(C)** Circular dichroism (CD) spectra of wild-type and R209E mutant.



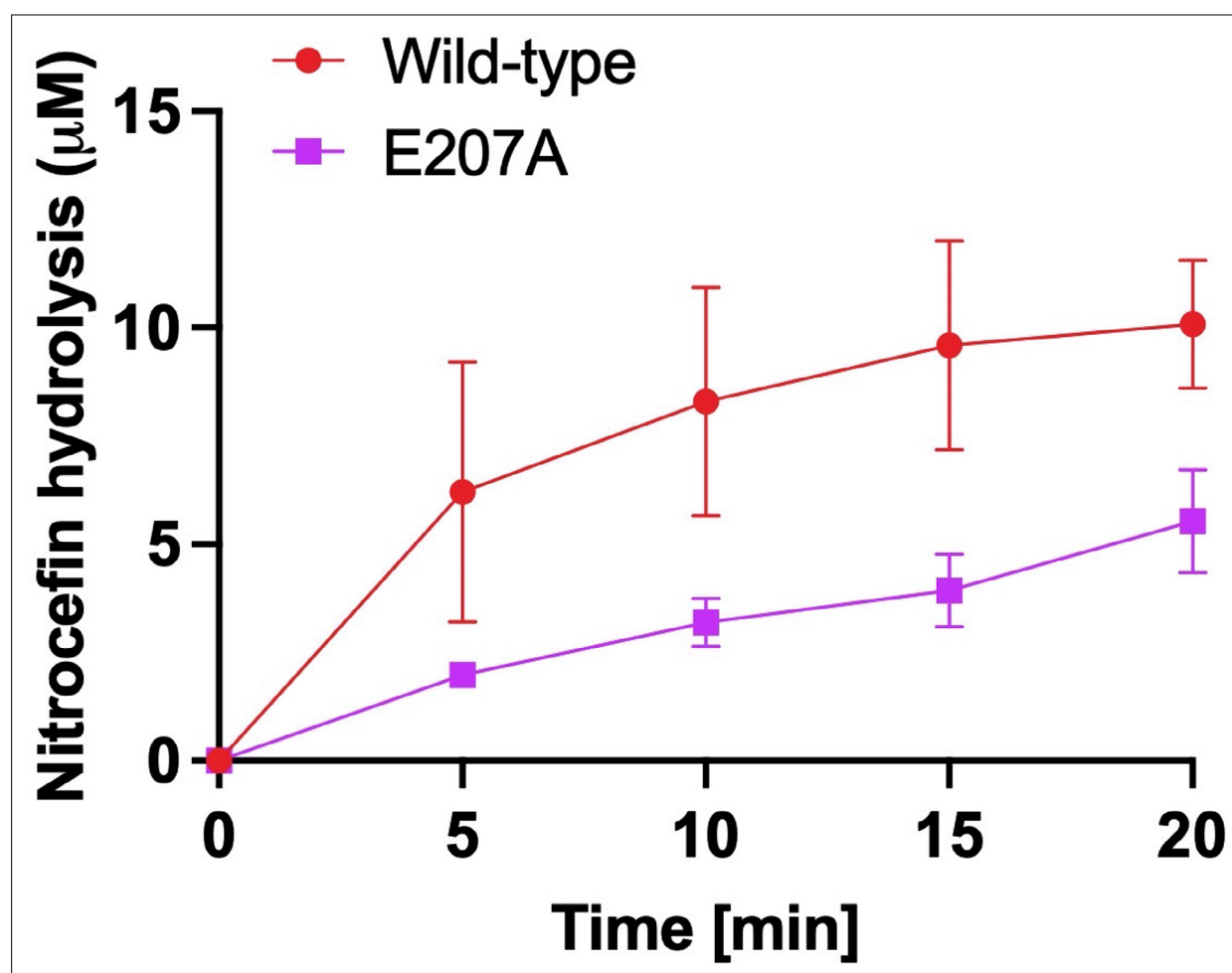


**Figure 2—figure supplement 1.** Chromogenic nitrocefin hydrolysis activity of wild-type Ldt<sub>M12</sub> and E207A mutant.

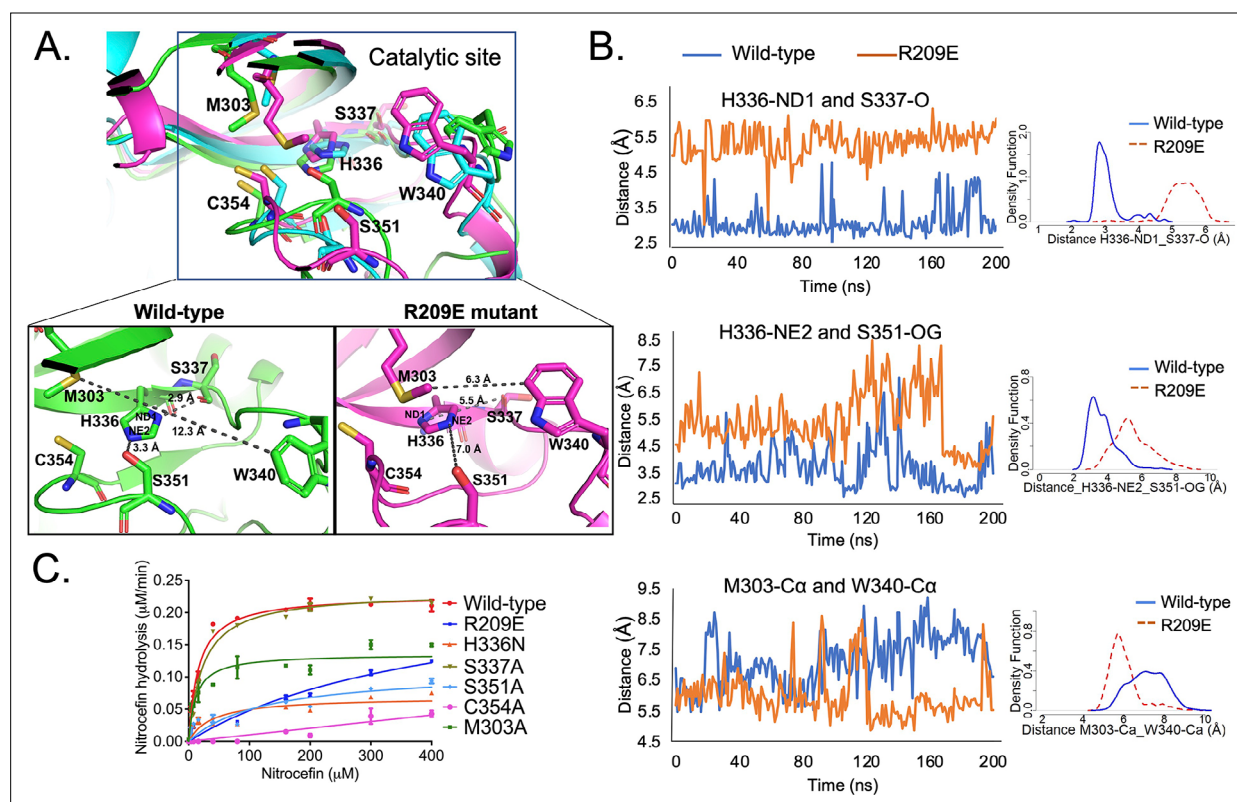


**Figure 3.** S-pocket crosstalk with the catalytic site of *Ldt<sub>Mt2</sub>*. **(A)** Superposition of molecular dynamic (MD) simulated structures of catalytic site of wild-type *Ldt<sub>Mt2</sub>* (146–408 residues, green) and the R209E mutant (146–408 residues, pink) at 150 ns trajectory along with a trajectory (cyan) at 0 ns. The inset shows a detailed view of the catalytic site of the wild-type protein and R209E mutant at 150 ns trajectory. **(B)** Dynamic distance analysis of key residue pairs vs. simulation time calculated from 200 ns of MD simulation run. A density function graph is also plotted. **(C)** Chromogenic nitrocefin hydrolysis activity of wild-type *Ldt<sub>Mt2</sub>* and different mutants with alterations in both the S-pocket and catalytic site.

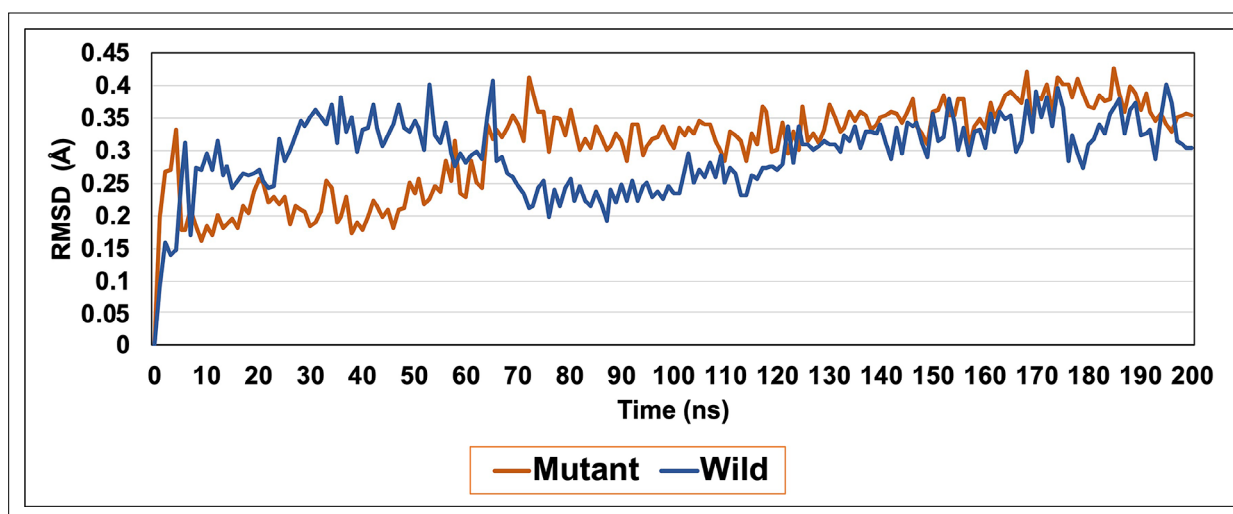


**Figure 3—figure supplement 1.** RMSD graph of wild-type Ldt<sub>Mt2</sub> (blue) and R209 mutant (orange) over the duration of 200 ns of molecular dynamic (MD) simulations.

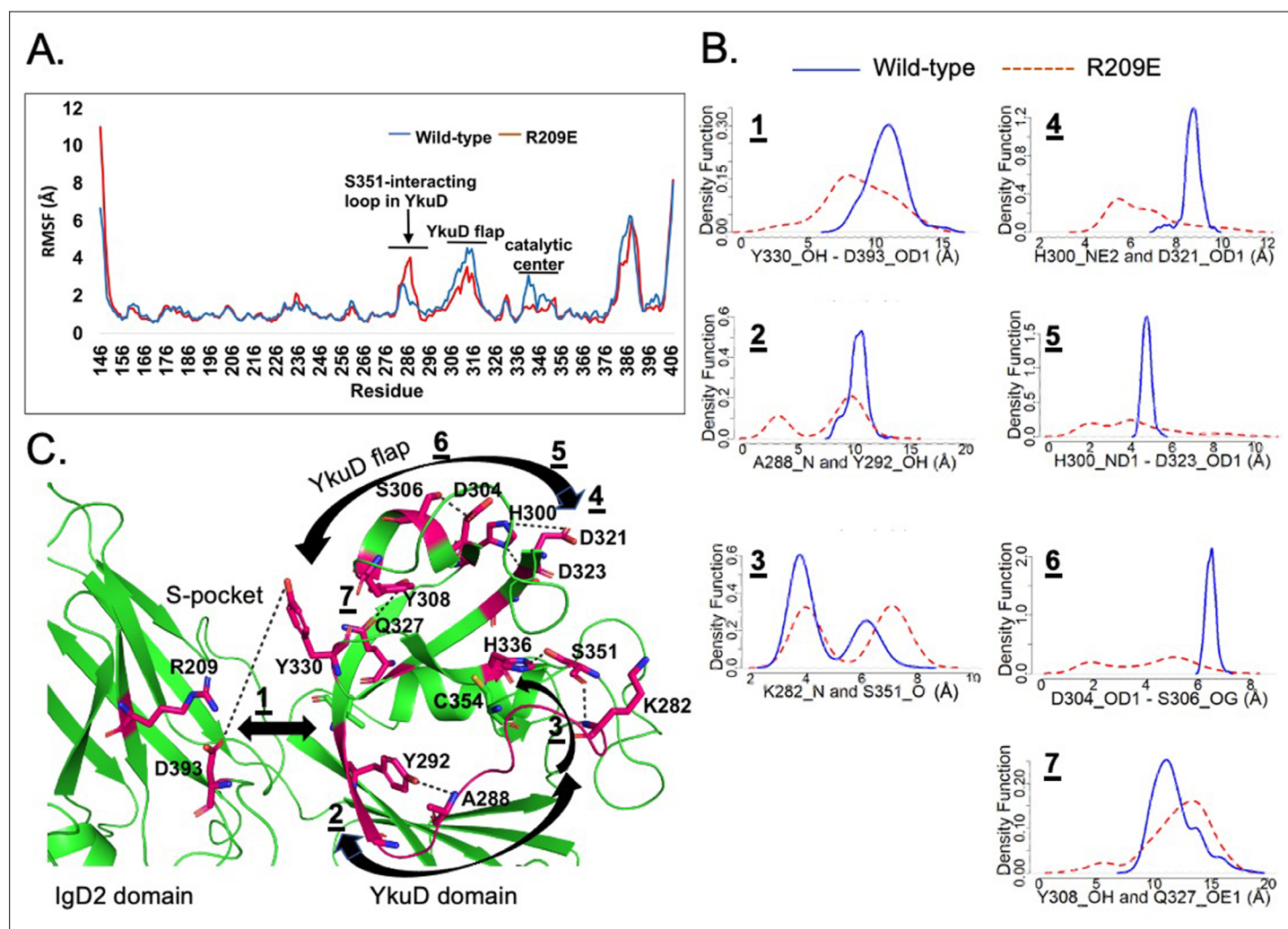


**Figure 3—figure supplement 2.** An analysis of dynamics in-between the S-pocket and catalytic site in *Ldt<sub>Mt2</sub>*. **(A)** Root mean square fluctuation (RMSF) graph of wild-type *Ldt<sub>Mt2</sub>* (blue) and R209 mutant (orange) over the duration of 200 ns of molecular dynamic (MD) simulations. **(B)** A density function graph of network analysis of dynamic distance between selected pair of amino acid residues in *Ldt<sub>Mt2</sub>*. **(C)** Structure of *Ldt<sub>Mt2</sub>* (green colour) with highlighted residue pairs (shown in stick model and pink colour) that undergo alterations in the dynamics subsequent upon mutation in R209 residue.

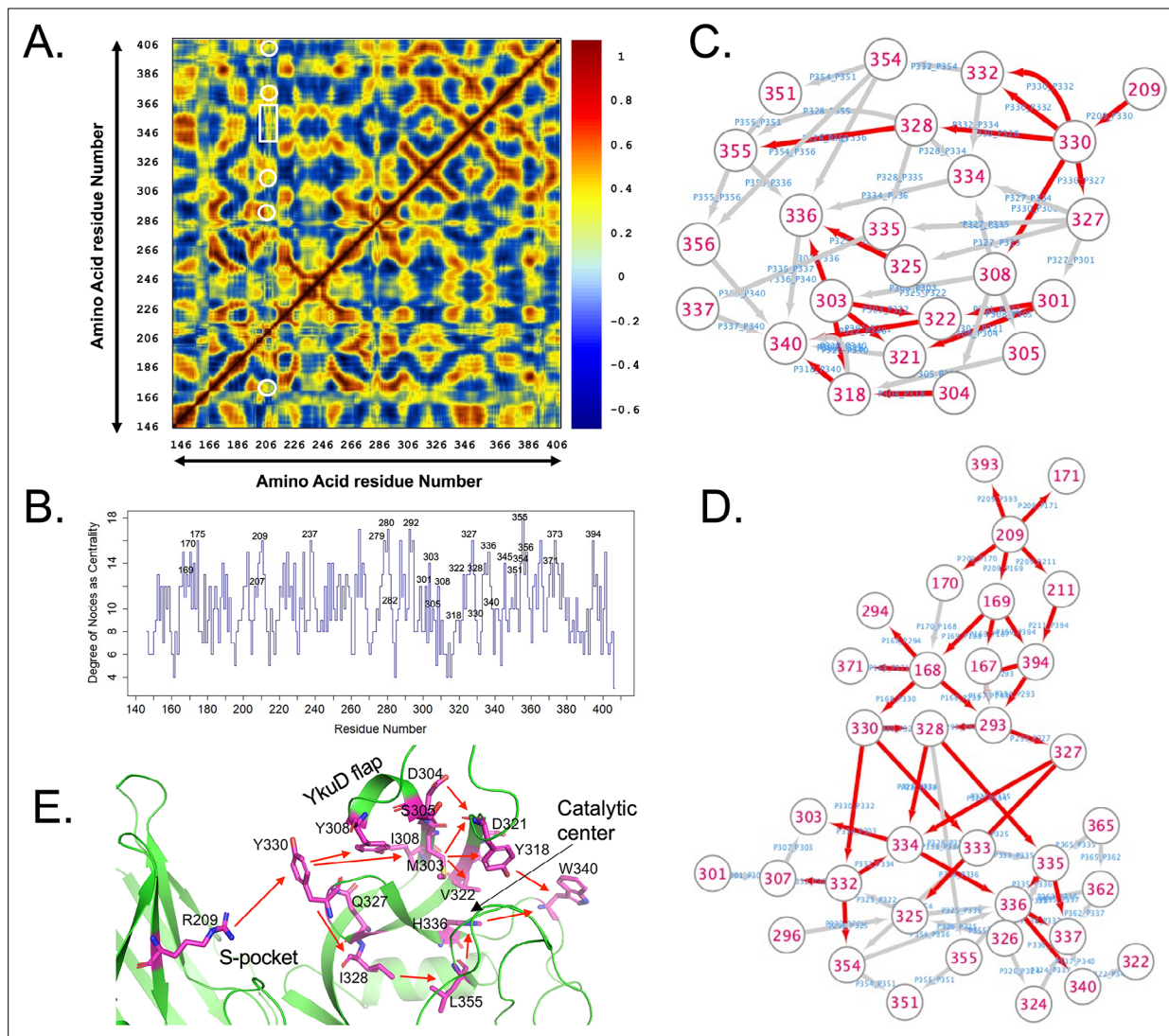


**Figure 3—figure supplement 3.** Network analysis of Ldt<sub>M12</sub> dynamics. **(A)** Plotted correlation map showing a coupling of dynamic motions between residues. Highlighted white boxes show positive correlation (>0 value) of R209 residue with other residues from the S-pocket and catalytic site. **(B)** Graph of centrality measure vs. each amino acid residue. The higher the centrality values, the more likely is the residue (node) important for the three-dimensional fold of the protein and network of interactions. **(C, D)** Network paths computed in cytoscape from the simulation of wild-type and R209E mutant protein from 209 residue towards catalytic site residues. Red arrows indicate edges with >6 threshold of betweenness. **(E)** Structure of Ldt<sub>M12</sub> representing the flow of network of allosteric communications from the S-pocket to catalytic site.



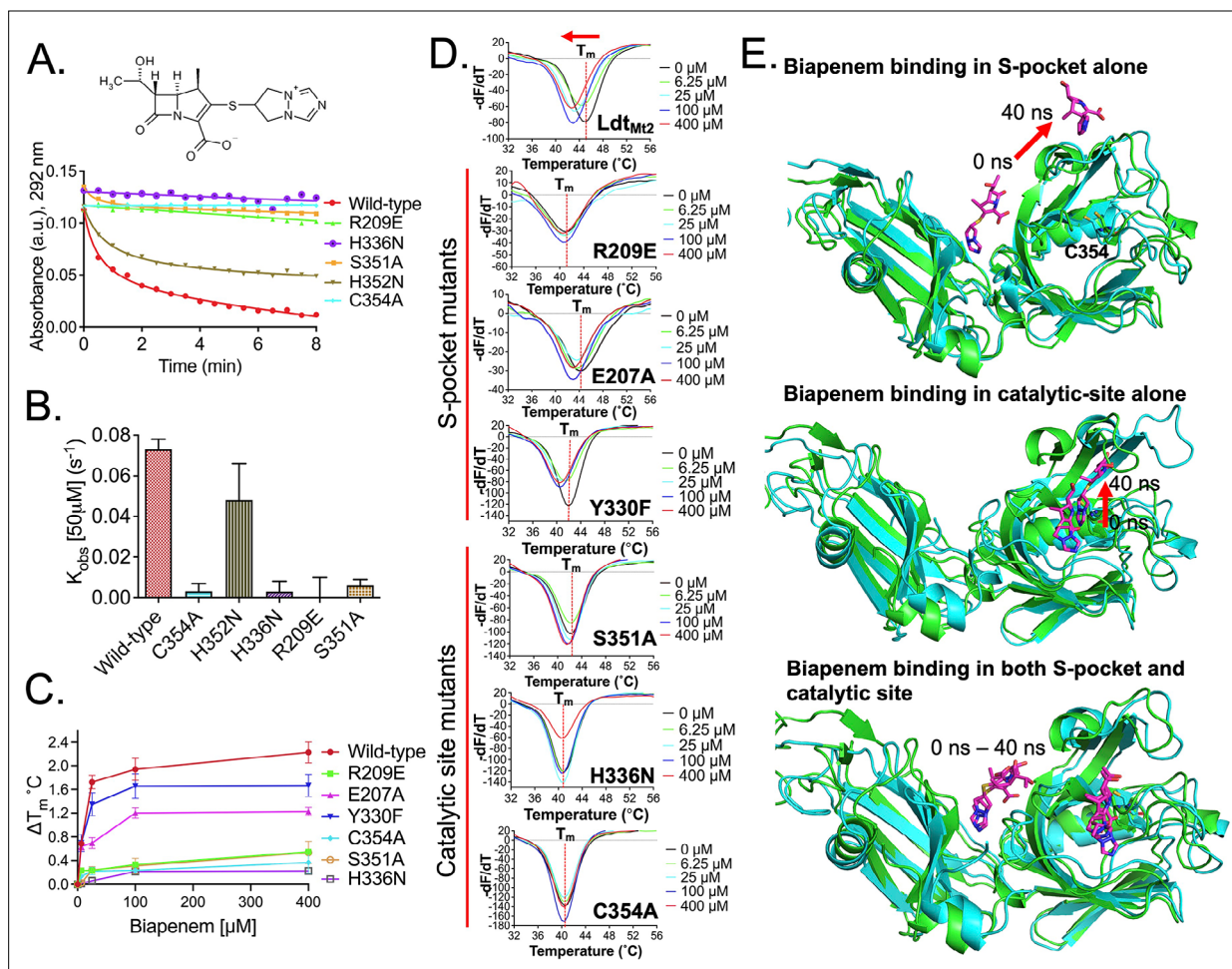


**Figure 4.** Role of the S-pocket and catalytic site in recognizing biapenem. **(A)** Acylation activity of biapenem with Ldt<sub>Mt2</sub> and mutants R209E, H336N, S351A, H352N, and C354A was monitored at 292 nm wavelength using UV–visible spectrophotometry. Maximum absorbance spectra of biapenem were found at 292 nm that was used to monitor decrease in biapenem concentration upon acylation with the Ldt<sub>Mt2</sub>. The chemical structure of biapenem is shown above the biapenem acylation graph. **(B)** Rate of acylation of 50 μM biapenem per second with Ldt<sub>Mt2</sub> and mutants. **(C)** ThermoFluor assays for binding of biapenem with Ldt<sub>Mt2</sub> and mutants R209E, E207A, Y330F, S351A, H336N, and C354A mutants. A change in melting temperature ( $\Delta T_m$ ) was plotted at y-axis versus the ligand concentrations at x-axis in GraphPad Prism software. **(D)** Differential fluorescence ( $-dF/dT$ ) graphs of ThermoFluor assay for Ldt<sub>Mt2</sub> and mutants. The dotted line indicates the  $T_m$ , and a red arrow indicates the direction of thermal shift. **(E)** Molecular dynamic (MD) simulations of Ldt<sub>Mt2</sub> in complex with biapenem. Ldt<sub>Mt2</sub> is represented in cartoon with green colour at 0 ns and cyan colour after running the MD simulations at 40 ns, and biapenem is represented in stick model with pink colour. The red arrow indicates the movement of biapenem to a second position revealed by the MD simulations after 40 ns trajectory.



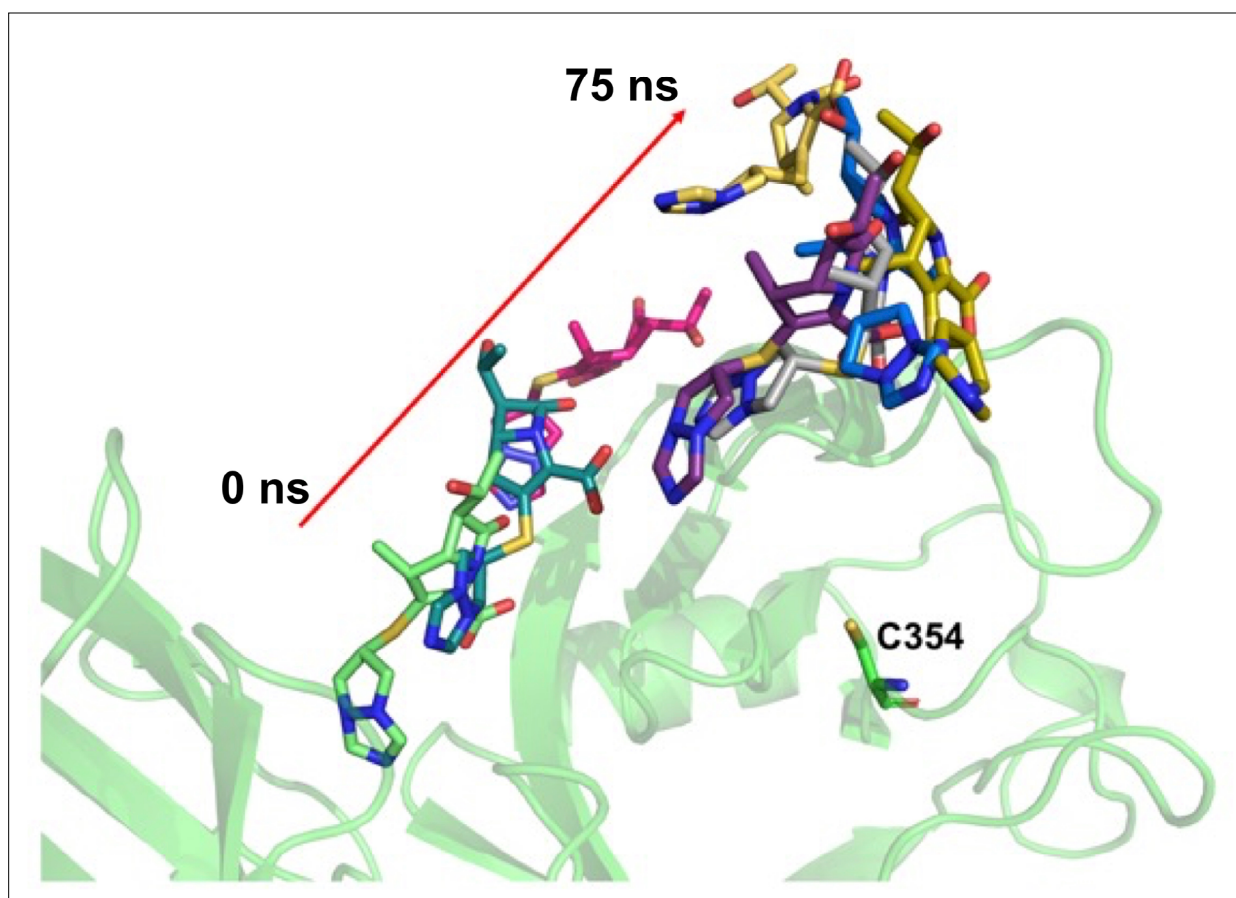


**Figure 4—figure supplement 1.** Molecular dynamic (MD) trajectory of biapenem bound in S-pocket alone in Ldt<sub>M12</sub>-Bia<sup>S</sup> structure. A red arrow indicates the direction of movement of biapenem during an overall 75 ns of MD simulation. Ldt<sub>M12</sub> is represented in cartoon in green colour and biapenem in various trajectories is represented in stick model.

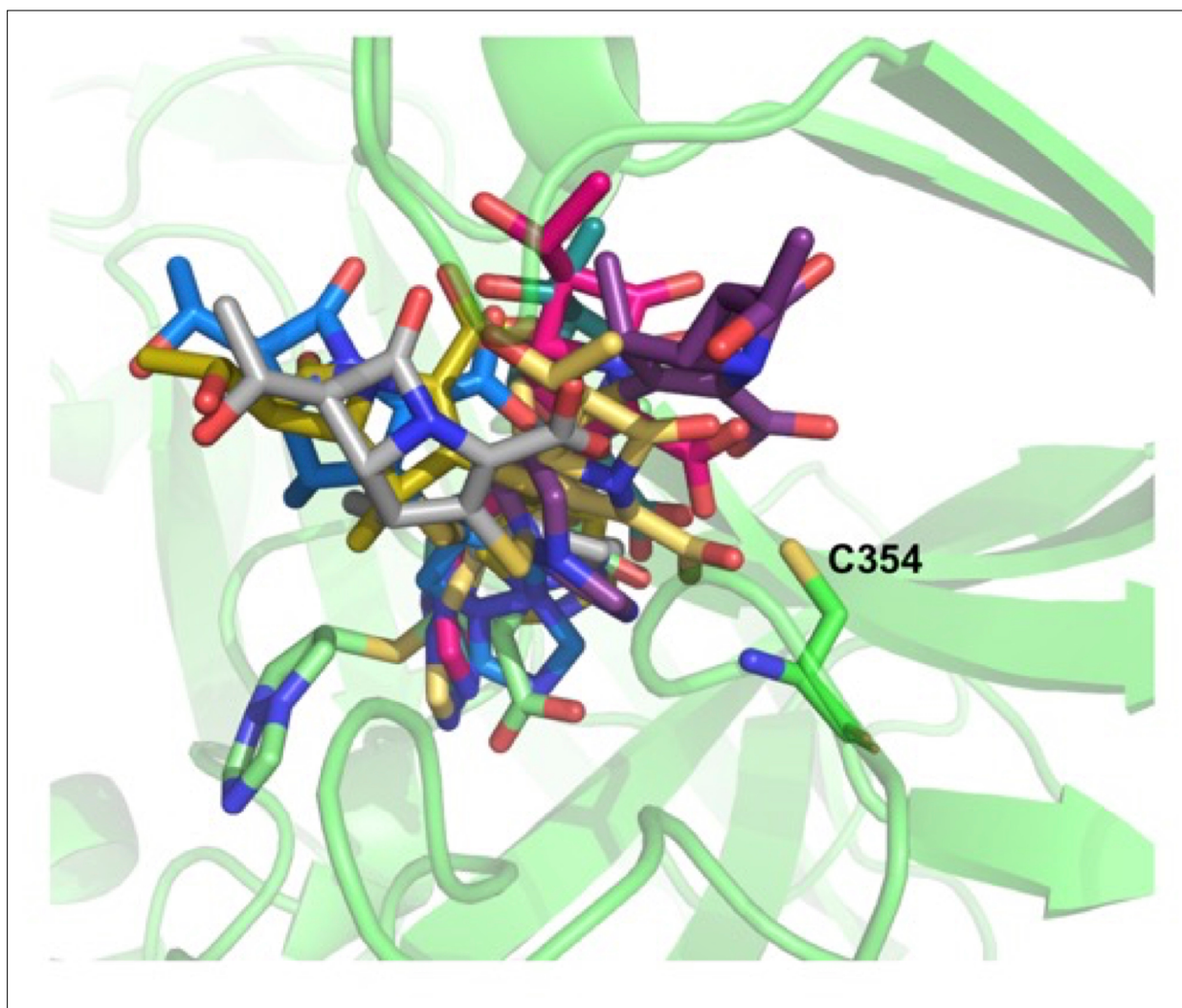


**Figure 4—figure supplement 2.** Molecular dynamic trajectory of biapenem bound in catalytic site alone in Ldt<sub>Mt2</sub>-Bia<sup>C</sup> structure. Ldt<sub>Mt2</sub> is represented in cartoon in green colour and biapenem in various trajectories is represented in stick model.

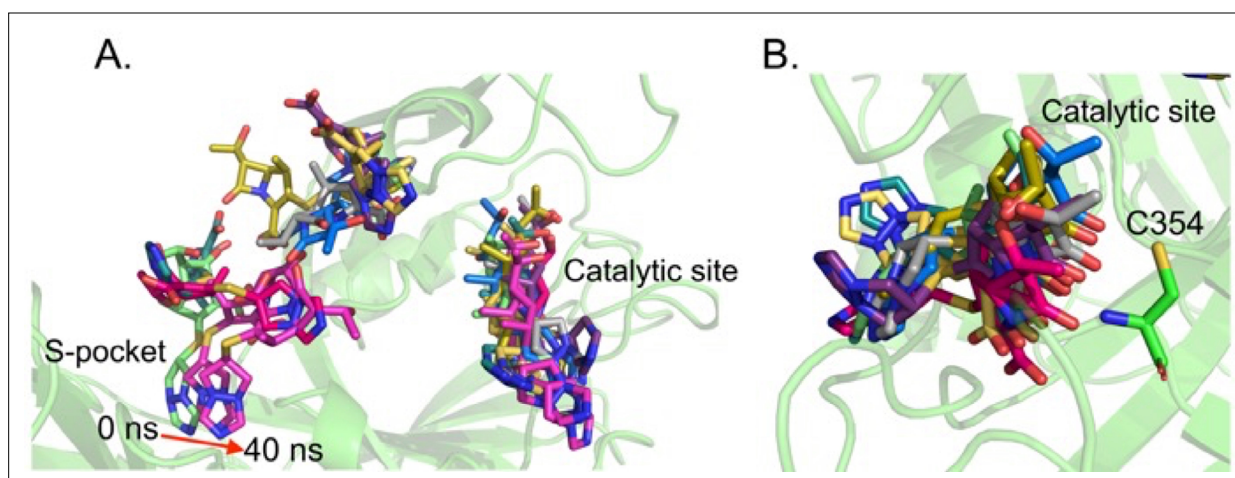


**Figure 4—figure supplement 3.** Molecular dynamic trajectory of dual biapenem bound in both S-pocket and catalytic site in Ldt<sub>M12</sub>-Bia<sup>S-C</sup> structure. **(A)** Snapshots of biapenem from both S-pocket and catalytic site. **(B)** Snapshots of biapenem from catalytic site. Ldt<sub>M12</sub> is represented in cartoon in green colour and biapenem in various trajectories is represented in stick model.

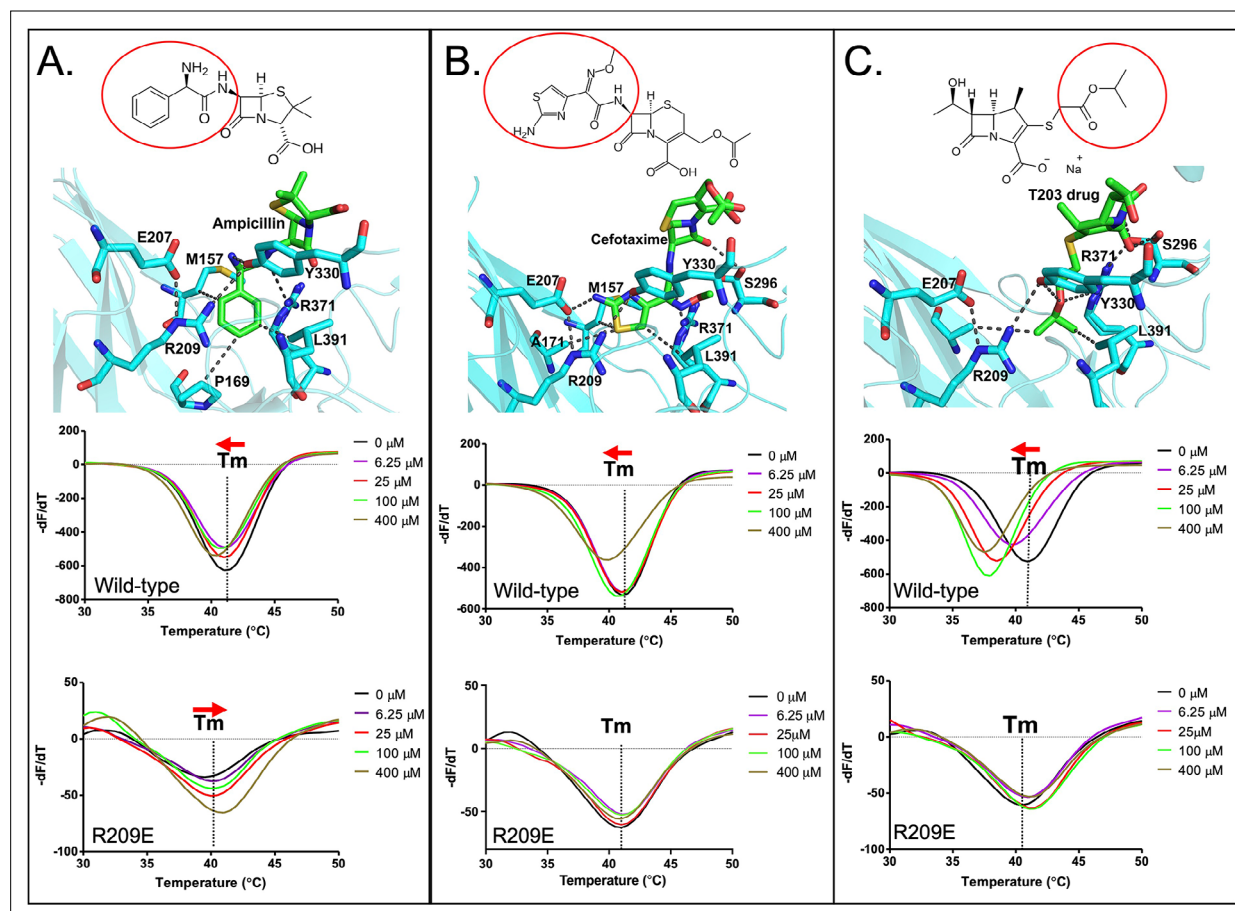


**Figure 5.** Binding of various subclasses of  $\beta$ -lactams to the S-pocket. **(A)** Top: ampicillin (stick model in green) bound to the S-pocket (cyan) of  $Ldt_{M12}$  through its R1 group side chain, 2-amino-2-phenylacetyl (red oval). Bottom: ThermoFluor assays for binding studies of ampicillin with wild-type  $Ldt_{M12}$  and the R209E mutant. **(B)** Top: cefotaxime (stick model in green) bound to the S-pocket (cyan) of  $Ldt_{M12}$  through its R1 group side chain, thiazol-4-yl (red oval). Bottom: ThermoFluor assays for binding studies of cefotaxime with wild-type  $Ldt_{M12}$  and the R209E mutant. **(C)** Top: the experimental carbapenem drug T203 (stick model in green) bound to the S-pocket (cyan) of  $Ldt_{M12}$  through its R3 group side chain, 2-isopropoxy-2-oxoethyl (red circle). Bottom: ThermoFluor assays for binding studies of T203 drug with wild-type  $Ldt_{M12}$  and the R209E mutant.

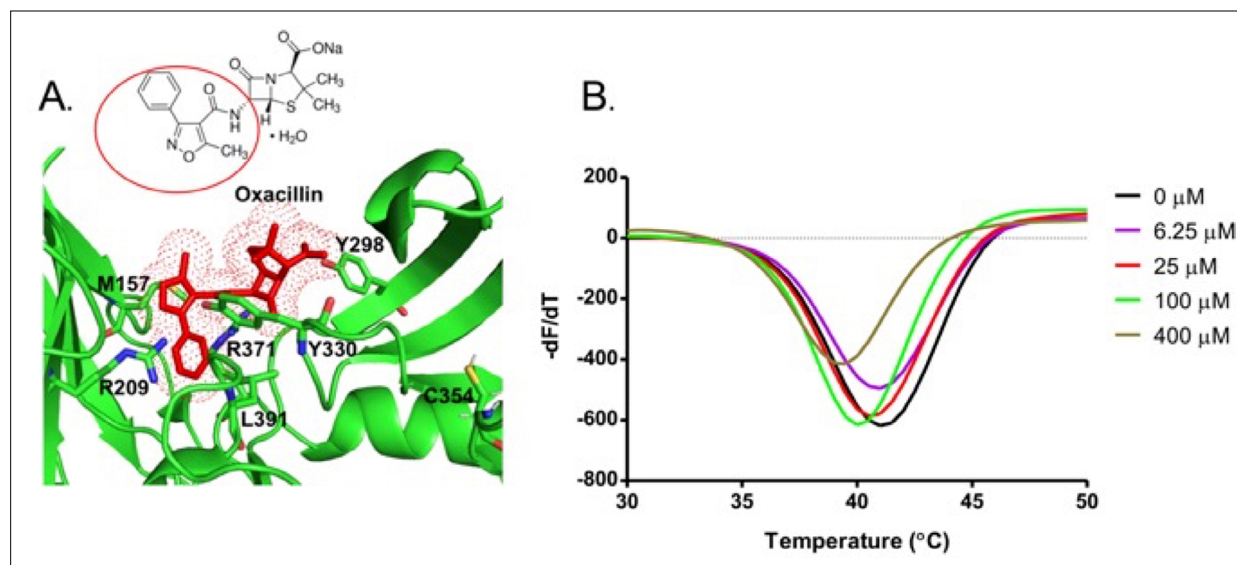


**Figure 5—figure supplement 1.** Binding of oxacillin drug to the S-pocket. **(A)** Oxacillin (stick model, red colour) bound into the S-pocket (green colour) of Ldt<sub>M12</sub> through R1 group side chain 5-methyl-3-phenyl-1,2-oxazole-4-carbonyl. 5-Methyl-3-phenyl-1,2-oxazole-4-carbonyl group is highlighted with red circle in the chemical structure of oxacillin. **(B)** ThermoFluor assay for binding studies of oxacillin with wild-type Ldt<sub>M12</sub>.



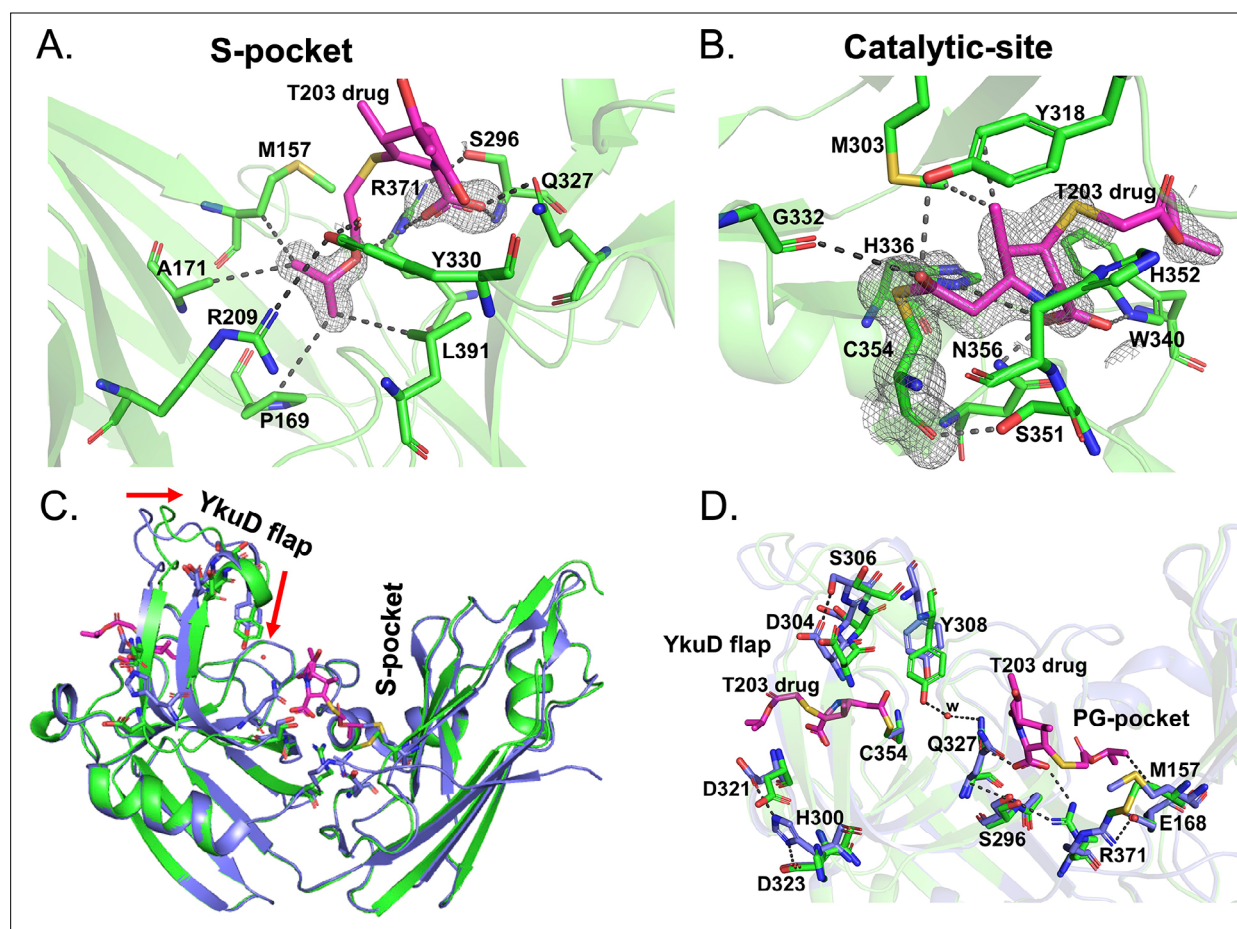


**Figure 6.** Structural studies of  $Ldt_{Mt2}$  with the experimental T203 carbapenem drug and allosteric conformation analyses. **(A)** The 2Fo-Fc map (contoured at  $1.0\sigma$ ) of the T203-R3 group side chain, 2-isopropoxy-2-oxoethyl (pink), modelled in the S-pocket of  $Ldt_{Mt2}$  in the crystal structure. **(B)** The 2Fo-Fc omit map (contoured at  $1.0\sigma$ ) of the full T203 structure (pink) modelled in the catalytic-site of  $Ldt_{Mt2}$  where it acylates the C354 residue of  $Ldt_{Mt2}$ . **(C)** Superposition of the  $Ldt_{Mt2}$ -T203 complex (green) with C354A catalytic mutant structure (PDB ID: 3TX4, blue). The red arrows indicate movements in YkuD flap upon T203 drug binding. **(D)** Residues that have undergone allosteric alterations upon T203 drug binding are shown with stick models.  $Ldt_{Mt2}$ -T203 complex residues are represented in green and the C354A catalytic mutant in blue.



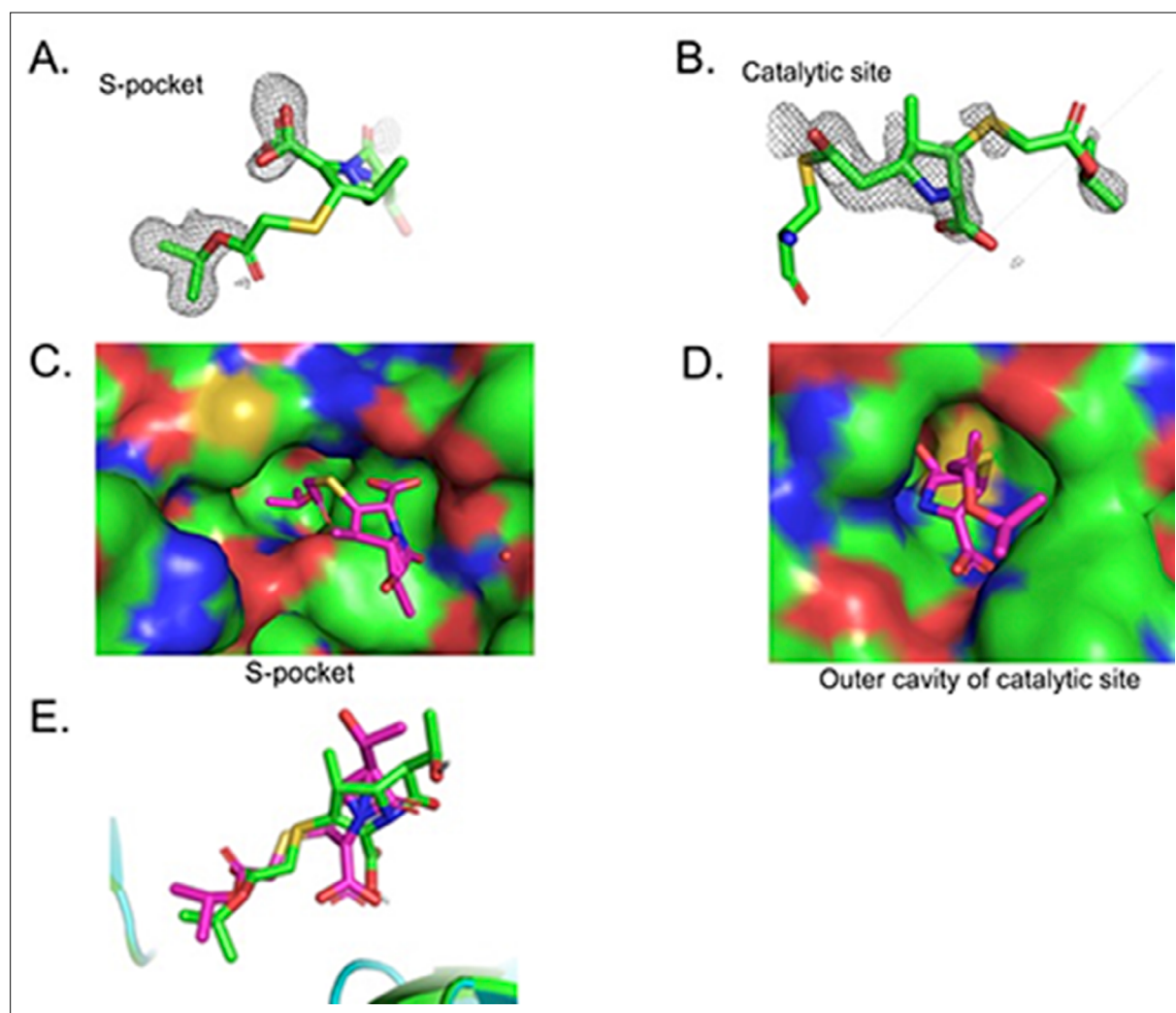


**Figure 6—figure supplement 1.** Crystal structure studies of binding of T203 drug in the S-pocket and catalytic site in *Ldt<sub>M12</sub>*. **(A)** Fo-Fc omit map calculated in the S-pocket contoured at  $3\sigma$ . **(B)** Fo-Fc omit map calculated in the catalytic site and contoured at  $3.0\sigma$ . **(C)** T203 drug modelled into the S-pocket of *Ldt<sub>M12</sub>* in the crystal structure. T203 drug is represented in stick model with green colour. **(D)** T203 drug modelled into the outer cavity of catalytic site of *Ldt<sub>M12</sub>* in the crystal structure. *Ldt<sub>M12</sub>* is represented in surface and T203 drug is represented in stick model with pink colour. **(E)** Superposition of T203 drug from docking result (green colour) with T203 drug from crystal structure (pink colour).

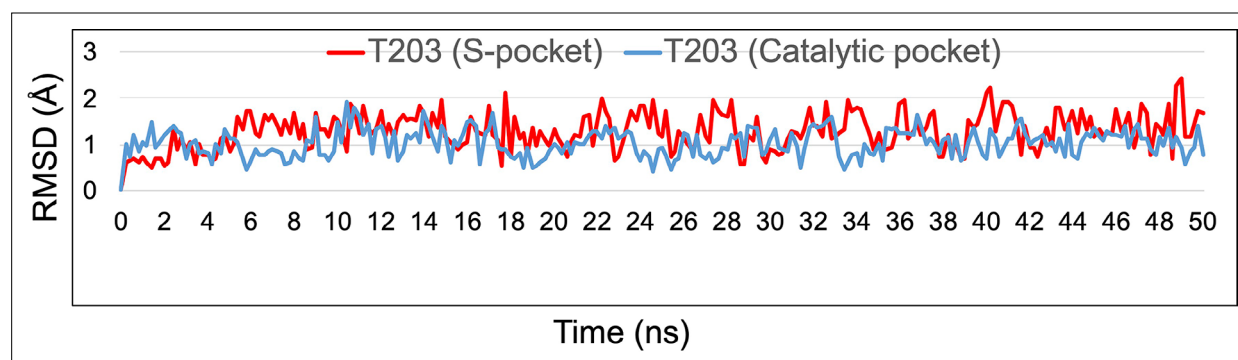


**Figure 6—figure supplement 2.** RMSD graph of T203 (S-pocket) (red) and T203 (catalytic-pocket) (blue) over the duration of 50 ns of molecular dynamic (MD) simulations in  $\text{Ldt}_{\text{M12}}\text{-T203}^{5\text{-C}}$ .

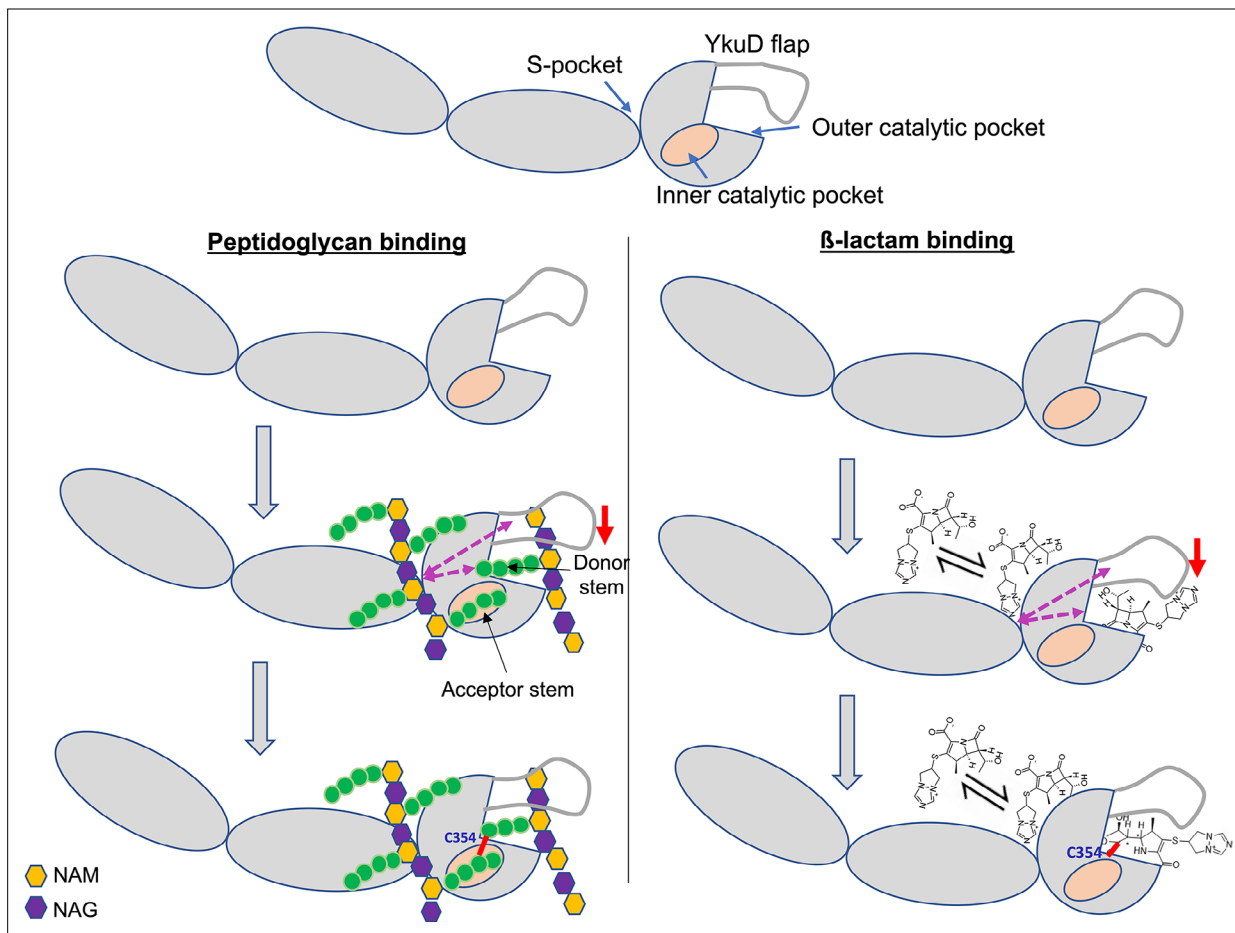


**Figure 7.** Model of dual  $\beta$ -lactam and/or dual peptidoglycan (PG) substrate binding in S-pocket and the catalytic site of  $Ldt_{M12}$  enzyme that is allosteric cooperative. Purple dotted arrows indicate pathways of allosteric communication and red arrow indicates movement of YkuD flap during  $\beta$ -lactam and/or PG binding. A small red line in the figure indicates a covalent bond between donor and acceptor stem peptides of PG chain or covalent bond between catalytic residue C354 and  $\beta$ -lactam.  $\beta$ -Lactam molecule indicated in the model is biapenem.

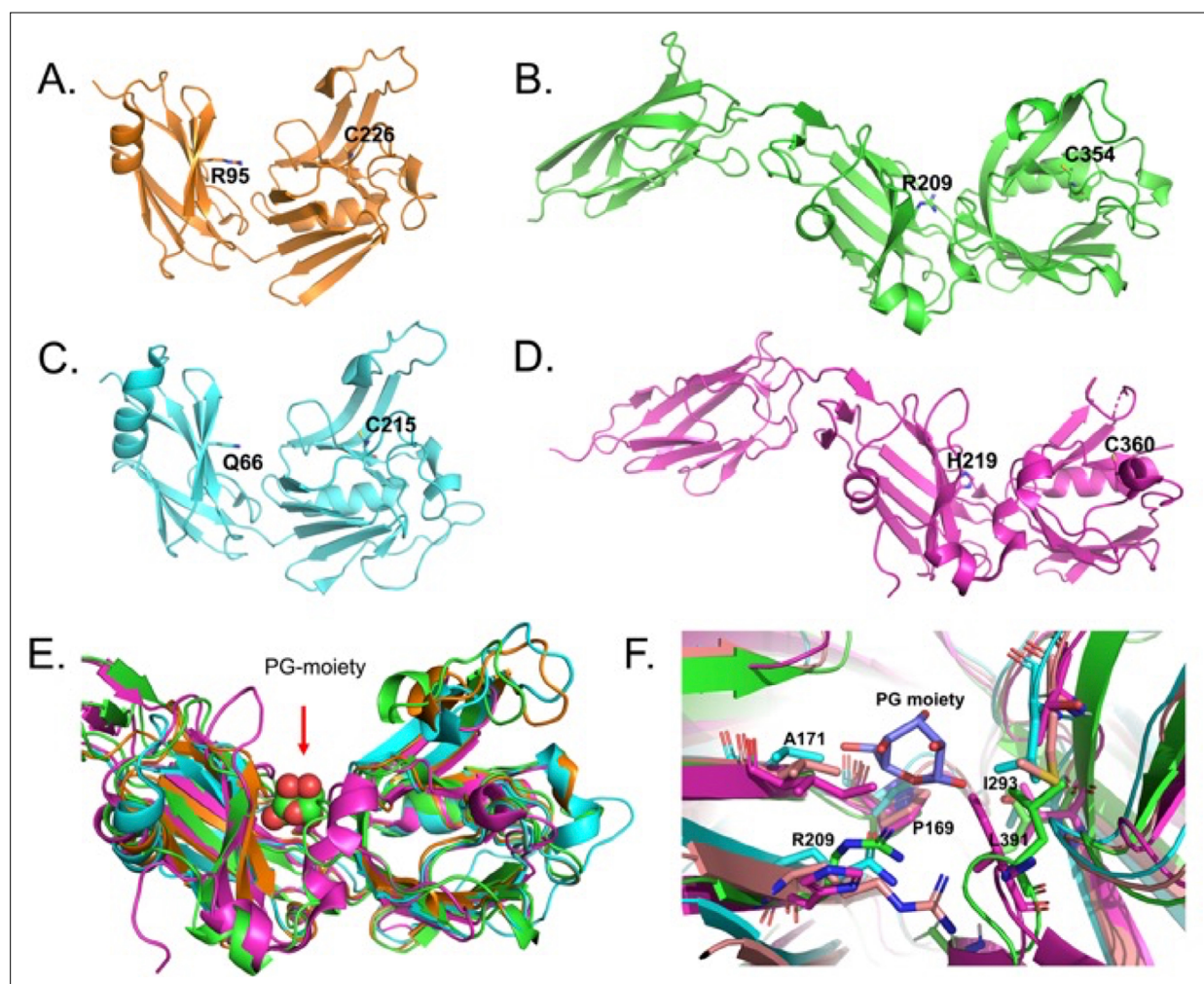


**Figure 7—figure supplement 1.** S-pocket in different L,D-transpeptidases from *Mycobacterium tuberculosis*. (A–D) Crystal structures of various LDTs, Ldt<sub>Mt1</sub> (PDB ID: 4JMN; orange colour), Ldt<sub>Mt2</sub> (PDB ID: 7F71; green colour), Ldt<sub>Mt3</sub> (PDB ID: 6D4K; cyan colour), and Ldt<sub>Mt5</sub> (PDB ID: 6D5A; pink colour). Highlighted residues in the crystal structures belong to S-pocket and catalytic site. (E) Superposition of various LDTs. Peptidoglycan (PG) sugar moiety bound across the S-pocket is shown in sphere model. (F) Superposition of the conserved residues in the S-pocket. PG sugar moiety is shown in stick model with blue colour.